Shoreline Change of the Northern Yellow River (Huanghe) Delta after the Latest Deltaic Course Shift in 1976 and Its Influence Factors

Authors: Zhang, Xiaodong, Zhang, Yexin, Ji, Yang, Zhang, Yawei, and Yang, Zuosheng

Source: Journal of Coastal Research, 74(sp1) : 48-58

Published By: Coastal Education and Research Foundation

URL: https://doi.org/10.2112/SI74-005.1

Journal of Coastal Research	SI	74	48–58	Coconut Creek, Florida	2016

Shoreline Change of the Northern Yellow River (Huanghe) Delta after the Latest Deltaic Course Shift in 1976 and Its Influence Factors

Xiaodong Zhang[‡#*], Yexin Zhang[‡], Yang Ji[‡], Yawei Zhang[‡], and Zuosheng Yang[‡#]

[‡] College of Marine Geosciences
Ocean University of China
Qingdao, Shandong 266100, P. R. China

[#] Key Lab of Submarine Sciences & Prospecting Techniques, MOE
Ocean University of China
Qingdao, Shandong 266100, P. R. China

www. cerf-jcr. org

www. JCRonline. org

ABSTRACT

Zhang, X. D.; Zhang, Y. X.; Ji, Y.; Zhang, Y. W., and Yang, Z. S., 2016. Shoreline change of the northern Yellow River (Huanghe) Delta after the latest deltaic course shift in 1976 and its influence factors. *In*: Harff, J. and Zhang, H. (eds.), *Environmental Processes and the Natural and Anthropogenic Forcing in the Bohai Sea, Eastern Asia. Journal of Coastal Research*, Special Issue, No. 74, pp. 48–58. Coconut Creek (Florida), ISSN 0749-0208.

222 high-quality Landsat satellite images were used in this study to extract the instantaneous shoreline positions on 22 sections of the northern Yellow River delta. Based on the instantaneous water line position data, a new statistical method for studying annual shoreline change was proposed. The annual shoreline movement of the northern Yellow River delta after the latest deltaic course shift in 1976 was obtained. The results showed that the shoreline on northern Yellow River delta was mostly undergoing a retreat back process since 1976 due to the river course shift, relative sea level change, regional marine hydrodynamic forces and the local engineering constructions. The influence of the Yellow River deltaic course shift in 1976 on the shoreline change mainly occurred in the first 20 years in 1976–1996 after the course shift, and was mostly limited within 10 km range around the abandoned Diaokou river mouth. The coastal engineering constructions caused decrease of the erosion area by 61 km^2, or 31% of the total erosion area. Most of the northern Yellow River delta was relatively insensitive to the relative sea level change except for the coast around sections S10 and S11; The annual shoreline movement due to the relative sea level change along most of the coast was only 1–3% of the actual annual shoreline movement; the total erosion area due to the relative sea level change was 9 km^2, or 5% of the actual erosion area. The coast erosion in the northern Yellow River delta was mainly influenced by the regional marine hydrodynamic forces, which gradually increase from west to east, resulting in gradually eastward increase of annual shoreline movement and slope steepness of the coast.

ADDITIONAL INDEX WORDS: *Yellow River delta, shoreline change, tidal height, slope coefficient.*

INTRODUCTION

Deltas are naturally dynamic coastal systems that are unique in their close links to both land-based fluvial and coastal ocean processes. In the presence of adequate fluvial sediment supply and minimal human influence, deltas generally maintain their integrity and/or continue to extend seaward (Sanchez-Arcilla *et al.*, 1998). More recently, pandemic construction of reservoirs and diversions of freshwater for consumptive uses have generally served to decrease the net sediment load of rivers (Nilsson *et al.*, 2005; Syvitski *et al.*, 2005). This decrease, along with isostatic loading factors, sediment compaction and accelerated subsidence of deltaic sediments resulting largely from local groundwater withdrawal and hydrocarbon extraction, has moved many deltas from a condition of active growth to a destructive phase (McManus, 2002; Milliman *et al.*, 1989). The hazard is compounded by the global historical trend in eustatic sealevel rise and predictions of increasing rates of sealevel rise over the next century (Church and Gregory, 2001).

As a young delta of a large river, the modern Yellow River delta has been formed since 1855 when the lower Yellow River channel migrated from the coast of the South Yellow Sea northward to the Bohai Sea. With annual sediment load of about 1×10^9 t the Yellow River used to be the second largest in the world in terms of sediment to the sea (Milliman and Meade, 1983). Two third of this huge sediment rapidly deposited in the subaerial delta area and subaqueous delta area, resulting in the most rapidly seaward prograding land area of China (Milliman and Meade, 1983). The deltaic channel and river mouth were silted strongly due to the rapid deposition of the highly concentrated suspended sediment, and caused 10 shifts of the deltaic course since 1855 and formed 11 delta lobes (Yin *et al.*, 2003). Each shift of the river deltaic course caused rapid accretion of the delta lobe around running river mouth, and rapid erosion retreat of the delta lobe around abandoned river mouth.

The present active Yellow delta lobe has developed since 1976, when the latest deltaic course shifted from the Diaokou course in the northern delta southward to the Qingshuigou course into the

DOI: 10. 2112/SI74-005. 1 received (27 Febuary 2015); accepted in revision (15 October 2015).

*Corresponding author: zxd@ouc. edu. cn

Laizhou Bay (Figure 1). The Qingshuigou course has been an active Yellow River course since 1976 up to present and the Qingshuigou Promontory has been accumulated (Bi *et al.*, 2014; Chu *et al.*, 2006; Cui and Li, 2011; Huangand and Fan, 2004; Kong *et al.*, 2015; Yin, 2003; Yu *et al.*, 2011; Zhou *et al.*, 2015). Yu *et al.* (2011) found that both the shoreline length and area of the Qingshuigou Promontory on the modern Yellow River delta extended overall in 1976–2009, but with decreasing rates in accordance with changes of runoff and sediment load. High increasing rate of shoreline length of 3.63 km/yr and quick area extension of 16.26 km^2/yr were observed in 1976–1985. Since 1996, the average increase rate of shoreline length and area decreased to 0.80 km/yr and 3.94 km^2/yr. The evolution of shoreline and change of area of the Qingshuigou Promontory are directly affected by the dramatic reduction of the runoff and sediment load to the sea, which are closely related to human activities in Yellow River drainage basin in the past half century. The results of Chu *et al.* (2006) showed the maximum accretion occurred at the head of the Qingshuigou Promontory where the shoreline advanced seaward over 20 km with a mean net accretion rate of 0.83 km/yr in 1976–1996, the shoreline at the head of the Q8 Promontory advanced seaward 7 km with a mean net accretion rate of 0.29 km/yr in 1996 –2000. Total area of the Qingshuigou and Q8 Promontories increased by 384.16 km^2 and 11.88 km^2, with mean net accretion rates of 16.4 km^2/yr and 3.03 km^2/yr. Cui and Li (2011) showed that the general pattern of accretion-erosion of the Qingshuigou Promontory was divided into four stages: rapid accretion stage (1976–1986), accretion-erosion adjustment stage (1986 – 1996), slow erosion stage (1996–2003), and slow accretion stage (2003–present). Zhou *et al.* (2015) argues that the 2000–2005 was transitional period, the growth rates of river mouth channels, shorelines and land area change from an increasing trend to a declining one.

The northern abandoned Diaokou Promontory has experienced significant erosion since 1976 due to lack of sediment supply from the Yellow River (Chen *et al.*, 2006; Chu *et al.*, 2006; Li *et al.*, 2000; Yin, 2003). Li *et al.* (2000) depicted three stages of evolution of the abandoned Diaokou subaqueous delta slope after lobe abandonment: rapid erosion stage (1976 – 1985), slow erosion stage (1985–1992) and erosion-accumulation adjustment stage (1992 – 1996). Chu *et al.* (2006) showed that the maximum erosion occurred at the head of Diaokou and Shenxiangou Promontories in 1976–2000, with mean net erosion rates of 290 and 190 m/yr, respectively, total area was reduced by 141.3 km^2 with a mean net erosion rate of 6.03 km^2/yr. And wave-induced alongshore current is the major driving force to transport sediment from eroded areas. Chen *et al.* (2006) concluded that Diaokou shoreline retreated 400m/yr in 1976–1984, and 200m/yr in 1984 – 1986, the abandon of Diaokou course is the main cause of strong coastal erosion.

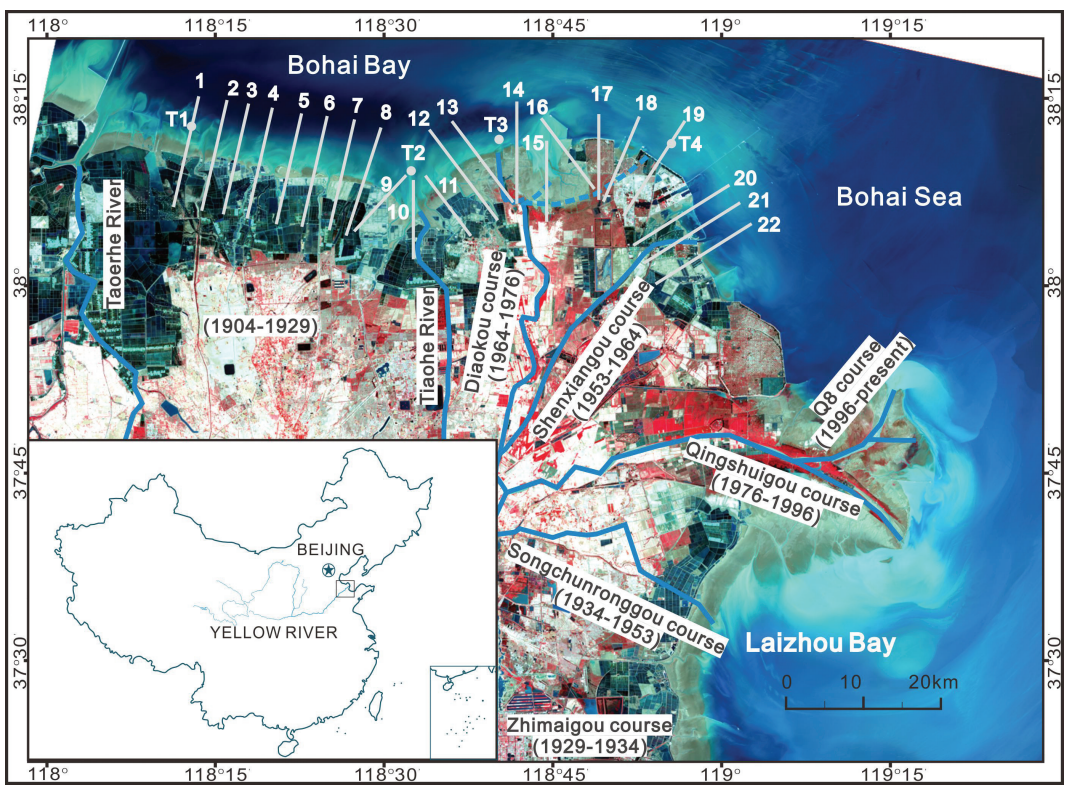

Figure 1. Study area, locations of 22 study sections and historical deltaic shifts of theYellow River course after 1904

Besides the deltaic course shift, the shoreline change can be influenced by the Yellow River sediment load to the sea, regional marine hydrodynamic forces, coastal engineering constructions and relative sea level change (RSLC). Yang *et al.* (2011) concluded that fluvial sediment discharge to coastal ocean areas plays a primary role in the erosion and accretion of deltas. Peng *et al.* (2010) estimated that water-soil conservation practices in the Yellow River Basin which are a major factor to the decrease of sediment load at Huayuankou gauging station account for 40% of the total amount of reduction, sediment trapping by reservoirs account for 30% of the total amount of reduction and 10% decrease is caused by human activities in the upper reaches, the remaining 20% decrease is attributed to precipitation decrease. Bi *et al.* (2014) showed that the Huanghe Water-Sediment Regulation Scheme and groins may partially contribute to the accretion of the active Yellow delta lobe. Chen *et al.* (2006), Wang *et al.* (2010) and Yang *et al.* (2011) concluded that the waves and tidal current are combined to be the dominant dynamic mechanism of coastal erosion in the northern Yellow River delta, the tidal residual current takes and transports the sediment outward, thus causing the sediment to wane in the coast. RSLC is very important to shoreline change. Higgins *et al.* (2013) showed that large deltaic aquaculture facilities can induce land subsidence of 1 m every 4 years, these rates exceed local and global average sea level rise by nearly 2 orders of magnitude and suggested that subsidence and associated relative sea level rise may present a significant hazard for Asian mega-deltas.

Previous studies on shoreline change of the Yellow River delta was mainly focused on the active Qingshuigou Promontory, and abandoned Shenxiangou and Diaokou Promontories, but less attention was paid to the shoreline change in this vicinity of the Bohai Bay, a comprehensive and systematic study of the Bohai Bay shoreline change has not yet been reported.

Owing to the Yellow River fluvial sediment reduction, frequent shift of the river deltaic course, RSLC, the impact of human activities as well as regional hydrodynamic forces, the modern Yellow River delta is experiencing radical changes. Although previous studies carried out extensive research to the shoreline changes of Yellow River delta, however, there are some important issues remained: 1) The quantity of the remote sensing images used in previous studies was not large enough and the duration of these images was not long enough to get the adequate statistical data for the shoreline change; 2) High tide lines or low tide lines are quite difficult to recognize on satellite images; 3) Although the instantaneous water lines can be recognized easily, the water level correction error cannot be ignored owing to the lack of accurate historical instantaneous water level data. Eventually, the shoreline change rates from different researchers were quite different, even the erosion-accretion stage divisions were different either. Therefore, the conclusions deduced from the data which was severely affected by errors were not conducive for accurate and quantitative analysis of historical shoreline changes, as well as for the analysis of the influencing factors.

STUDY AREA

The Yellow River delta has developed since 1855 when the river lower course swung back from the South Yellow Sea to the Bohai Sea. The river deltaic course has shifted 10 times in the Yellow River delta since it reentered the Bohai Sea, forming 11 delta lobes (Yin *et al.*, 2003). The river deltaic course was mainly located between the Taoer River and Tiaohe River in 1904 – 1929, between the Songchunronggou course and Zhimaigou course in 1929 – 1953; the course shifted to the Shenxiangou course in 1953–1964; and then shifted to the Diaokou course in 1964–1976. The latest shift occurred in 1976 when the river course shifted southeastward to the Qingshuigou course, resulting in the formation of the present Qingshuigou river delta lobe and the abandoned Diaokou river delta lobe. A minor course shift occurred in 1996 and the river course moved northeastward to the present Q8 course, leaving the Qingshuigou river mouth abandoned (Figure 1).

The study area is located in the west to the Taoerhe River and east to the Shenxiangou course, facing mostly to the Bohai Bay, and partly to the central Bohai Sea (Figure 1). The tidal regime off the Yellow River delta is dominated by an irregular semidiurnal tide with a mean range of 0.8–2.6 m. An amphidromic point of the M2 tide is located in the east of the study area (Between S20 and S21). The lowest tidal range of 0.8 m occurs near the amphidromic point of the M2 tide, and it gradually increases westward and southward (Hu and Cao, 2003).

The climate in the study area has distinct seasonal variability associated closely with monsoon activity. The prevailing northerly winds are much stronger in winter than the dominant southerly winds in summer. Winds with a maximum velocity of >11 m/s come primarily from the NW and NE in winter, and waves are generated mainly by local winds in the Bohai Sea. The prevailing wave direction is from the NE, and the maximum significant wave height is 5.2 m in the winter (Zang, 1996). The wave height in winter period from November to March is significantly higher than that in the rest months of the year as the result of the strong northerly wind. The residual current, driven by winds, in the surface layers is approximately 20–30 cm/s southward in winter and weaker northward in summer. The residual current is in a form of compensatory current with a speed of 5–15 cm/s in the near-bottom layers (Pang and Si, 1979; Zhang *et al.*, 1990).

The surface sediment is composed mainly of silt and clayey silt, with a grain size of less than 0.01mm (Qin *et al.*, 1985). The intertidal flat forms a wide beach that extends 2 – 7 km seaward with minimum slope about 0.03 ~ 0.04%.

DATA SOURCE

Satellite images

Total 222 scenes of high-quality satellite images in 1976–2013 including multi-temporal remote sensing data of Landsat Multi-spectral Scanner (MSS), Thematic Mapper (TM) and Enhanced Thematic Mapper (ETM+) satellite images were collected and used in this study. They were freely acquired from the Earth Resources Observation and Science Center (http://glovis.usgs.gov/) and Chinese Academy of Sciences (http://www1.csdb.cn/).

The criteria for selecting the satellite images are that the shorelines of the northern Yellow River delta can be clearly distinguished visually on the satellite images.

Estimation of tidal level

The tidal records of tide gauges near the study area did not provide sufficient information to determine the instantaneous height of the waterline (Liu *et al.*, 2013), therefore, a hydrodynamic tidal model was used to determine the height of the sea surface. Matsu-

moto *et al.* (2000) developed a global ocean tidal model (NAO. 99b) for 16 major short period constituents by assimilating about five years of Topex/Poseidon altimeter data into the numerical hydrodynamic model, the tidal height were calculated at four separate positions T1-4(Figure 1).

METHODS

Though strictly defined as the intersection of water and land surfaces, for practical purposes, the dynamic nature of shoreline and its dependence on the temporal and spatial scale at which it is being considered results in the use of a range of shoreline indicators. These proxies are generally one of two types: either a feature that is visibly discernible in coastal imagery or the intersection of a tidal datum with the coastal sections. Recently, a third category of shoreline indicator has begun to be reported in the literature, based on the application of image processing techniques to extract proxy shoreline features from digital coastal images that are not necessarily visible to the human eye(Boak and Turner, 2005).

In this study, 222 Landsat satellite images were selected to extract the instantaneous shoreline positions on 22 sections on the northern Yellow River delta. Statistical method is used to analyze the instantaneous shoreline position sequences to get shoreline historical change rates in the northern Yellow River delta after the latest river deltaic course shift in 1976 for avoiding the large image recognition error of using the fuzzy high tide line or low tide line, and for avoiding the water level correction error of using simulated tidal height replacing historical water level. Finally, we discussed the influences of the river course shift, engineering constructions, RSLC and regional hydrodynamic forces on the shoreline changes on the northern Yellow River delta.

The insufficiency of previous studies on shoreline change by using satellite images

Previous studies often adopted the concepts of high tide line, low tide line or instantaneous water line when extracting shoreline from satellite images. Although the high tide line and low tide line are not affected by the historical water level, but its characteristics on satellite image are not clear, which would lead to wrong image interpretation (Boak and Turner, 2005; Chen and Chang, 2009). Automatic identification of high tide line and low tide line using computer is very difficult, and can only be interpreted by human. And, different personnel's interpretation results are often different, eventually led to the big differences of shoreline changes between different researches. Instantaneous shoreline position represents the position of the land-water interface at one instant time rather than 'normal' or 'average' conditions(Boak and Turner, 2005). It changes continually with time because of beach variation, and it also changes because of the dynamic nature of water levels at the coastal boundary, such as waves and tides, so it is problematic using instantaneous shoreline to represent the actual shoreline, especially when the errors induced by tidal variation are more than the errors induced by spatial resolution, tidal affects must be considered (Guariglia *et al.*, 2006). Instantaneous shoreline position change caused by actual water level variation was now usually solved by water level correction (Chen and Chang, 2009; Liu *et al.*, 2013). But due to the lack of historical water level, the simulated tidal height instead of historical water level to correct the instantaneous shoreline position was usually used in the previous studies. However, except for astronomical tidal height, historical water level is also associated with the winds and waves, sea level seasonal change etc. So using simulated tidal height replacing actual water level to correct shoreline position will inevitably bring in errors, especially when the beach is flat, the water level error will be greatly enlarged and passed to shoreline position, thus, over a large area of beach slopes less than 1∶500, it is significant that the study of moderate-resolution images with large numbers of historical data sources (such as Landsat images) to detect shoreline variability and erosion-accretion trends (Ekercin, 2007; Mason *et al.*, 1997).

The methods used in this paper

22 sections along the coast of the northern Yellow River delta were designed with ~3 km interval perpendicular to the shoreline avoiding the local river mouth. Section 1-9(S1-9) are located between the Taoerhe River and Tiaohe River, S13-14 are located on the side of Diaokou course, S10, S15 , S16 and S18 are located on the coast of landward recessed, S17-19 are located on the northeast cape, and S20 - 22 are located by the Shenxiangou course(Figure 1).

222 collected satellite images were processed following steps described as follow to study shoreline change on each section.

The first step is Image synthesis. The standard false-color composite method combining bands of 4, 3 and 2 (Landsat1-3 MSS bands of 7, 6 and 5) as Red, Green and blue was used.

The second step is histogram equalization to get clearer image (Wang *et al.*, 2006). Histogram equalization is a useful and common method for efficiently enhancing the characteristics of some brighter or darker imagery. The batch command of ERDAS9. 2 software was used to complete the histogram equalization operation of all 222 images.

The third step is geographic correction. By calculating the mean RGB values of corresponding pixels, we got a mean image of all the 222 images. The objects with sharp edges on both XY directions such as reservoir corner, river bend and road intersection etc. on the mean image as control points were used. Then each image was registered to the mean image. The root mean square error of the transformation was not permitted to exceed 0. 55 pixels according to Chu *et al.* (2006).

Then, we use the method of computer aided decision making to obtain the instantaneous shoreline position on each section. That is, firstly the computer provides a possible instantaneous shoreline position on every section by using canny edge extraction algorithm (Canny, 1986). A 5×5 Gaussian filter was applied to convolve with the image, and the position with maximum edge gradient on each section was used as the alternative instantaneous shoreline position. After ward we decided whether to accept, modify or delete (if the image is too obscure) the position through human-computer interaction. Instantaneous shoreline position on satellite image is very clear compared to high tide line and low tide line, and through human-computer interaction, the misjudgment of computer was eliminated, the results are more reliable compared to the traditional methods.

Fifth, the farthest instantaneous shoreline position to land in all images of each section was found. That is, on each section, we can get 222 instantaneous shoreline positions in all the 222 images at most, and through computing the distances of all the positions to the endpoint on land of each section, the maximum is "the far-

thest instantaneous shoreline position from the land". Then we record the distance of current instantaneous shoreline position to the farthest instantaneous shoreline position as instantaneous shoreline position (ISP), onshore (+)/offshore (−).

Finally, the changes of ISP are mainly composed of long term (inter annual) and short term (monthly/days) components in study area. The long term change is mainly caused by coastal erosion and RSLC, the annual shoreline movement (ASM) was obtained by using regression analysis of ~222 ISP data versus year, which can be used to measure the shoreline's long term change, also onshore (+)/offshore (−). Then, the de-trended instantaneous shoreline position (DISP) was obtained after removing the long term change from ISP sequence to study the short term change mainly caused by tide and wave etc. The beach slope was obtained by using regression analysis of ~222 DISP data versus simulated tidal height.

The statistical analysis of 222 satellite images which can greatly reduce the defect of low/moderate satellite image resolution, is helpful to get high accuracy shoreline change rates and beach slope. Compared with the results from the methods which only use two or several images to calculate shoreline change rate and beach slope, the results derived by the method introduced in this paper are more precise.

RESULTS

Instantaneous shoreline positions (ISPs) of 22 sections in 1976−2013

According to the aforementioned methods, the ISPs of 22 sections in 1976−2013 were established (Figure 2). The ISPs of S1 and S2 slightly decreased over time or remain the same in long-term, indicating the coast near S1 and S2 is stable. The ISPs of S3 − 22 increased with time gradually, indicating the coastal erosion occurred. The ISPs of S3−11 increased monotonously during the whole period, and the long-term change of the ISPs of S12−22 can be divided into two stages. The ISPs of S12, S13 and S15 increased quickly before 1996 but slow down after 1996 with fluctuated range decrease. The ISPs of S14, S16−22 can be divided into two stages as well, but the dividing time was not fixed (Figure 2). We found that the engineering construction was the major factor for causing the two stages of ISPs change in S14, S16−22: the ISPs increased quickly before engineering construction, but increased slower or kept constant after that.

Annual shoreline movements (ASMs) of 22 sections in 1976−2013

The ASM of each section was calculated according the stage-dividing time shown in Figure 2 respectively and the results were shown in Figure 3 and Table 1. The ASMs of S1−8 have highly linear positive correlation with each section's zonal distance from S1. The ASMs of S9−11 were significantly lower than that of the adjacent S8 and S12. The ASMs of S12−15 in 1976−1996 were larger than that in 1997−2013. The ASM of S13 in 1976−1996 was up to 251 m and is the largest. The ASMs of S16−20 were significantly reduced after engineering construction. The ASMs of S21 − 22 decreased slightly after engineering construction. The ASMs of S16−17, S19 and S22 decreased to 0 after engineering construction.

The ASMs of S1−8, S12 (1997−2013), S13, S15 and S16−20 (before engineering construction) were highly linear-positively correlated with each section's zonal distance from S1.

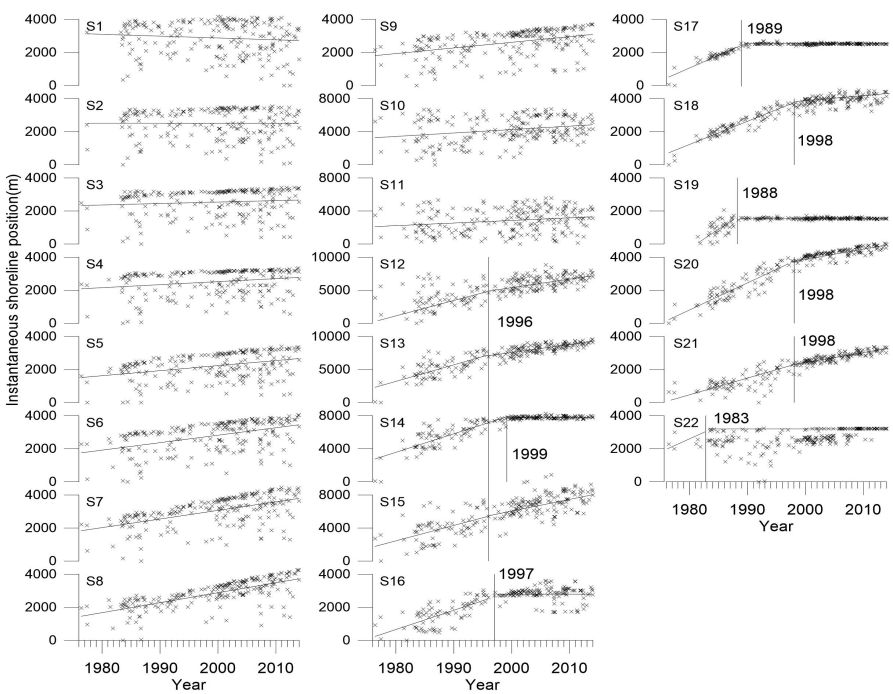

Figure 2. Instantaneous shoreline positions of 22 sections in 1976−2013

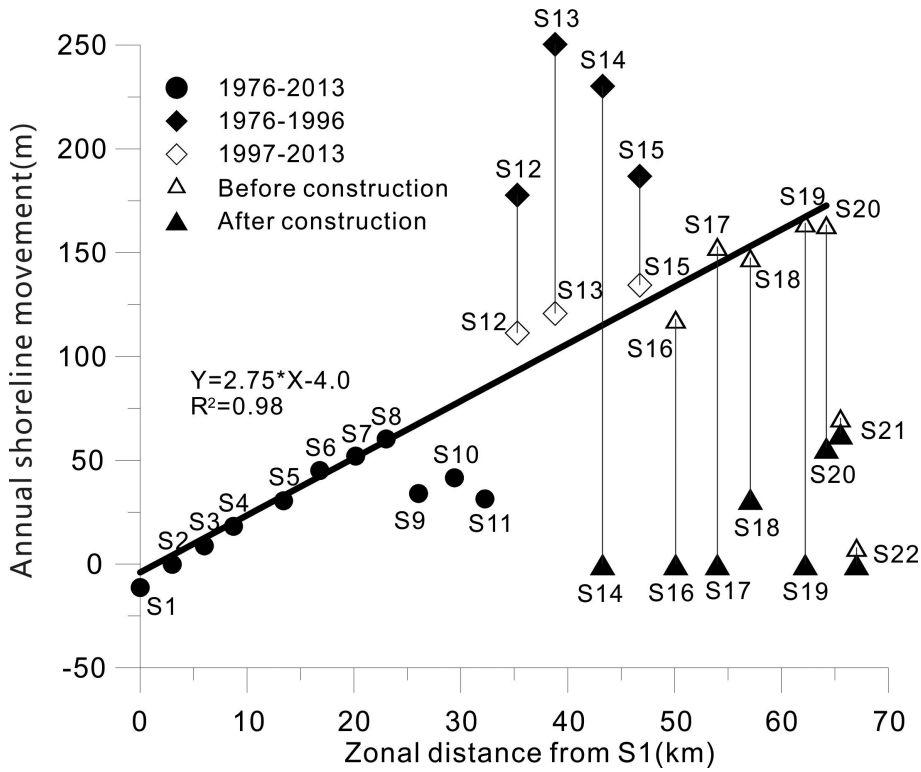

Figure 3. Annual shoreline movements of 22 sections in 1976–2013

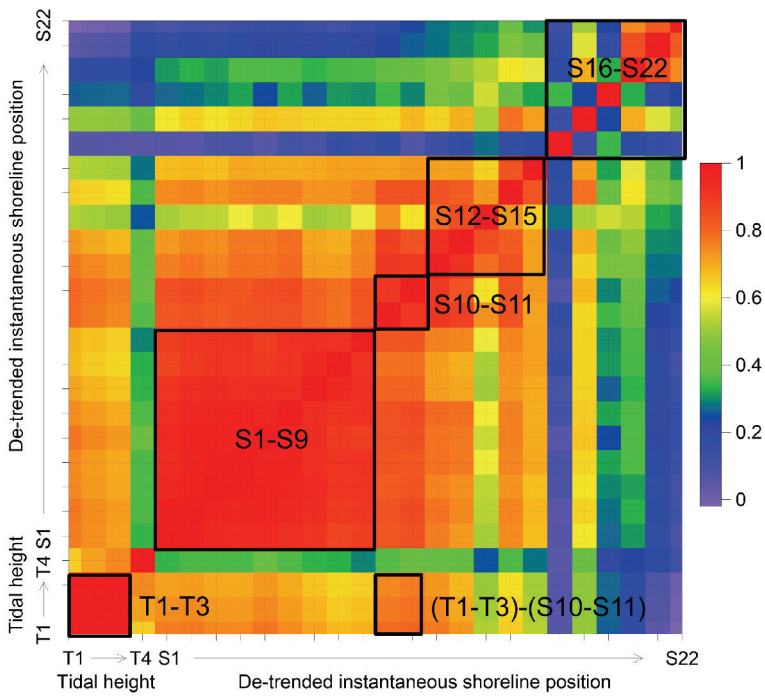

Figure 4. The correlation coefficients of de-trended instantaneous shoreline positions and tidal heights. T1–T4 are tidal heights of T1–T4; S1–S22 are de-trended instantaneous shoreline positions of S1–S22

The correlation coefficients between de-trended instantaneous shoreline positions (DISPs) and tidal heights

The DISPs were obtained after removing the long term change of ISPs, and the tidal heights at T1-4 (Figure 1) were obtained by using NAO. 99 b tide prediction model contributed by Matsumoto *et al.* (2000) due to the lack of historical water level observation data in the study area. The correlation analysis results are shown in Figure 4. The correlation coefficient was marked by the color of rectangles in this figure: the red square (correlation coefficient =1) means completely related, and the light blue square (correlation coefficient =0) means completely unrelated.

All the correlation coefficients in Figure 4 are ranged from 0 to 1, no negative correlation. There are several high value areas of correlation coefficients, including average value of 0.99 for T1 - T3; 0.85 for S1 - S9; 0.88 for S10 - S11 and 0.85 for S12 - S15. The S16 - S22 area is of medium correlation coefficients with average value of 0.62.

Correlation coefficients between tidal height of T4 and all DISPs are weak, with an average value of 0.34. As to T1 - T3, the average correlation coefficient is 0.62 of S1 - S9, 0.74 of S10 - S11 (the highest); 0.36 of S12 - S15 (poor) and 0.12 of S16 - S22 (the worst), respectively.

Slope coefficients (SCs) of 22 sections

SCs of sections S1-19 can be calculated from the regression analysis of DISPs versus tidal heights respectively. As to S20-21, for they are next to the M2 amphidromic point, the correlation coefficients between the tidal heights and DISPs are poor. However, the DISPs of S20-22 correlated well with the sea level heights computed from the DISPs and SCs of S10 and S11, so the SCs of S20, S21 and S22 was computed using the computed sea level heights replacing the simulated tidal heights.

Owing to the significant difference in high tide beach and low tide beach, the SCs on high tide beach and low tide beach of S1-9were calculated, respectively (Figure 5A). The SCs of S12-22 in different periods were also different and calculated corresponding to the periods as well. The results are shown in Figure 6.

The high tide beaches of S1-8 were steep with average SC of 108, and the low tide beaches were gentle with average SC of 1991, respectively. The beaches around S10-11 were the most flat with average SC of 2652. The beaches of S12-15 became steeper since 1996 with decreasing SCs. The SCs of S14 and S16 -22 were affected by the engineering construction with decreasing SCs after engineering construction. SCs of S14, S17, S19 and S22 reduced to 0 after the engineering construction, indicating that the beaches disappeared. The SC of S15 was significantly larger than SCs of adjacent sections. SCs of S1-9 in low tide beach, S12-13 in 1997-2013, S16-20 before engineering construction had good linear negative relationship with each section's zonal distance from S1.

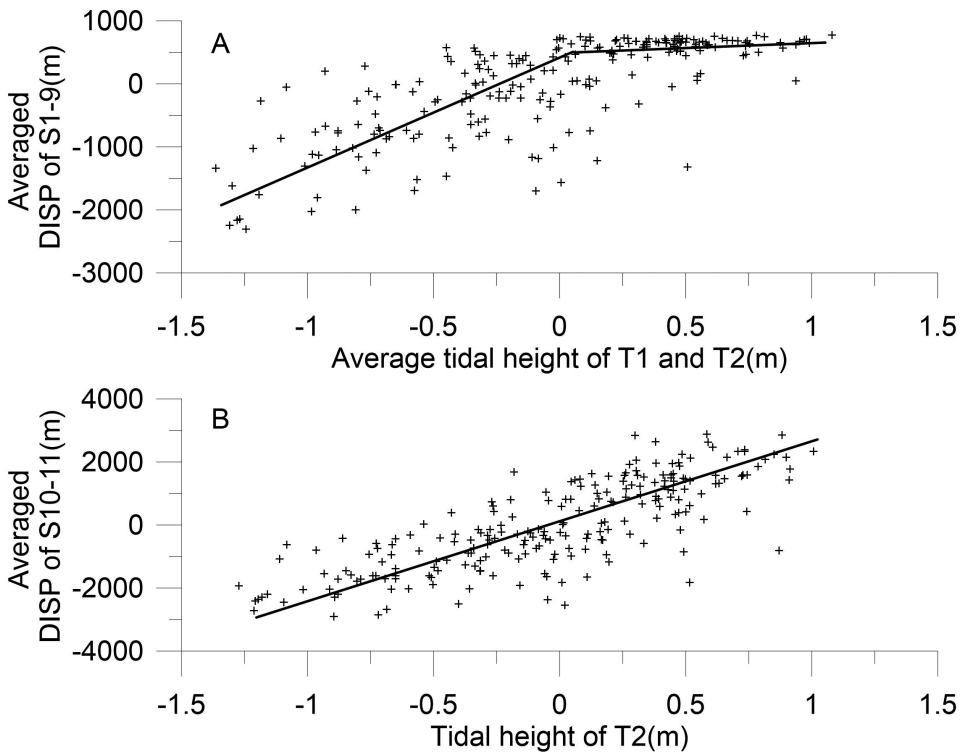

Figure 5. Calculation of slope coefficients

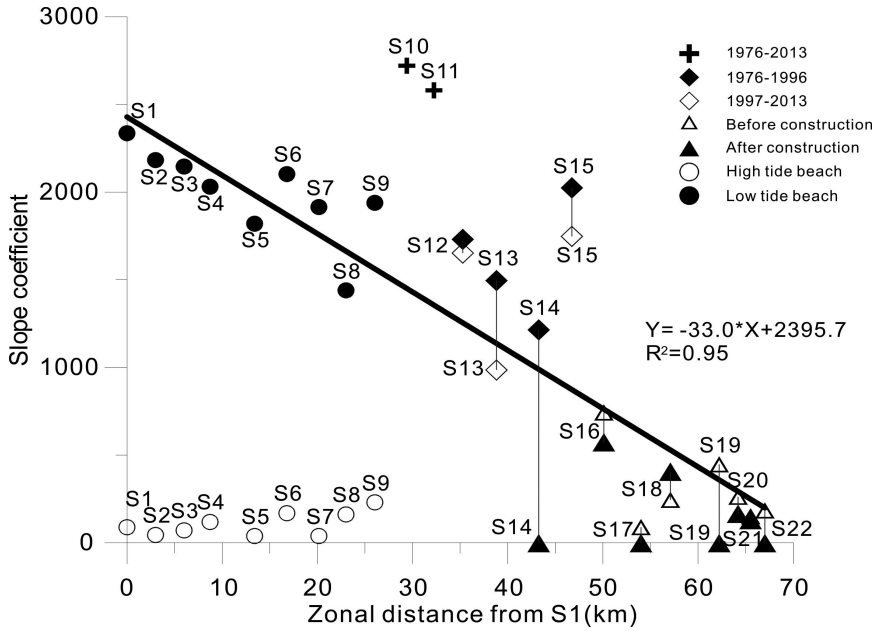

Figure 6. Slope coefficients of 22 sections

DISCUSSION

Shoreline change near the Diaokou mouth since 1976

Both sides of the coast near the Diaokou mouth experienced erosion process with time-dependent rate since 1976 as the deltaic course shifted from Diaokou course and the huge sediment supply was canceled. The coast erosion was fast in 1976–1996, in 20 years after the 1976 course shift. The most intensive coastal erosion in the study area happened in the coast around the Diaokou mouth. For example, the strongest erosion occurred along the nearest two sections to Diaokou, namely, the S13 and S14 with ASMs of 251 m and 230 m in 1976–1996, respectively. ASM of S13 in 1997–2013 decreased to 121 m, reduced by about 52%. ASMs of S12 and S15 which area little farther from Diaokou mouth(~7 km) reached as high as 178 m and 210 m in 1976–1996, respectively, then reduced by about 36% to 112 m and 135 min 1997–2013, respectively.

Coastal erosion of S12–15 was accompanied by its beach slope steepening. SC of S13 decreased from 1497 to 987, reduced by 34%. And SCs of S12 and S15 reduced by 5% and 14%, respectively. The ASM and SC of other sections far away from Diaokou mouth are not notably changed with time.

The Yellow River deltaic course shift in 1976 has strong influence on the shoreline changes in 1976–1996, in 20 years after the 1976 course shift, and the most affected area was limited within 10 km around the Diaokou mouth.

The influence of engineering construction to shoreline change

A road near S16 leading to the offshore oil platform was built in 1988 and begin to influence shoreline movement since 1996. The presence of road weakened the wave energy near S16 and protected the coast from erosion. Therefore, the ASM of S16 decreased gradually from 117 m to 0 since 1996 and with steeper beach slope.

Coastal dikes near S17, S19 and S22 were built in 1988, 1987 and 1976, respectively. The dikes stopped the shoreline change completely, and the fluctuant ISPs of S17 and S19 became stable since 1988 and 1989, soon after the dikes' built. The dike near S22 was built far away from low tide line in 1976, since then, the low tide line gradually moved onshore until arriving at the foot of the dike near S22 in 2009, the beach was no longer exposed (SC =0) since then.

Breakwaters near S18, S20–21 built in 1998 slowed the coastal erosion immediately, resulting in decrease of the ASMs and beach steepening.

S19–20 located on the coast near Shenxiangou course (1953–1964) where accumulated massive sediment and affected by the enhanced tidal currents and waves around the northeast salient corner of the delta. The ASMs of S19–20 were larger before the engineering construction, but the ASM of S19 reduced to 0 and the ASM of S20 reduced 65% after the engineering construction. S21 is far from the salient corner, the construction of the breakwater on the coast by S21 has a minor impact on coastal erosion, and the decrease of the ASM after the construction if the breakwater was little, too.

The ASM of S14 was large in 1976–1996 which is mainly contributed by the river course shift, and the ASM reduced to 0 since 1999 owing to the construction of the road leading to the off shore oil platforms. Among all the sections, S14 had the largest difference of ASM between two periods; it was caused by the superposition of two factors: the engineering construction and river course shift.

Engineering construction was the main reason which made the ISPs of S16–22 change in two stages, based on the type and posi-

tion of engineering building, its impact on coastal erosion is also different. Road and dike can completely stop the movement of shoreline once the low tide line moved to the foot, and breakwater can slow down the movement of shoreline immediately.

Table 1. *The engineering constructions on the northern Yellow River delta since* 1976

Location	First date seen in the satellite images	The year began to slow down the movement of shoreline	Types
S14	1999/4/6	1999	Road
S16	1988/6/9	1996	Road
S17	1988/6/9	1989	Dike
S18	1998/5/5	1998	Breakwater
S19	1987/3/4	1988	Dike
S20	1998/5/5	1998	Breakwater
S21	1998/5/5	1998	Breakwater
S22	1976/6/2	1983	Dike

The influence of relative sea level changes to shoreline change

The rate of sea level rise was 2.9 mm/yr in 1980–2013 according to the China Sea Level Bulletin (2013) edited by the State Oceanic Administration, and was higher than the global average. Yang and Shi (1999) and Yang (2002) estimated the RSLC off the Yellow River delta in the past few decades was 4.8 mm/yr which was notably higher than that in most Chinese seas.

According to the RSLC estimation of 4.8 mm / yr and the SCs derived in this paper, the ASMs caused by RSLC for S1–9, S10–11, S12–16 and S17–22 were about 0.5 m, 13 m, 6 m and 1 m, or 2%, 36%, 3% and 1% of the gross ASM, respectively. The beaches near S10–11 are relatively flat, and shoreline change affected by RSLC were the greatest. The beaches of other sections were steep, the shoreline changes affected by RSLC were small, only 1–3% of the total amount. RSLC was not the main influence factor for the erosion of the northern Yellow River delta.

The influence of coastal morphology to shoreline change

Part of eroded sediment from the protruding Promontories is transported into the concave coast, generally smoothing the coast (Chu *et al.*, 2006). S9–11 located near the mouth of the Tiaohe River, where the shoreline landward recessed, the landward recessed coast can slow the strength of hydrodynamics forces (including tides and waves), slow down the erosion of coast, resulting in the smaller ASMs of S9–11 than adjacent S8 and S12.

Shoreline near S15 is also landward recessed, but since it is located near Diaokou course, the ASM of S15 was greatly influenced by the Yellow River course shift in 1976, so the influence of morphology was not notable to the shoreline near S15.

Shoreline near S17–19 was smooth before 1989, however, owing to the construction of dike by S17 and S19, the shoreline near S18 retreated back about 1.5 km from 1989–1998, and the shoreline near S17 and S19 became seaward protruding since 1998. The protruding coast of S17 and S19 weakened the waves spread to S18, and slowed down the shoreline erosion near S18 (ASM decreased), beach became flatter with increasing SC.

The influence of hydrodynamic factors to shoreline change

In order to assess the influence of hydrodynamic forces to shoreline change alone, the other influential factors such as river diversion, engineering construction as well as morphology need to be eliminated. So we selected the ASMs of S12, S13 and S15 in 1997–2013 which were less affected by river course shift, the ASMs of S16–20 before engineering construction, and the ASMs of S1–8, exclude S9–11which were greatly influenced by coastal morphology and S21–22 which located on the eastern side of the Yellow River delta, and made a regression analysis using the aforementioned selected ASMs with each section's zonal distance from S1, and get the following regression equation:

$$ASM = 2.75 * Distance - 4.0$$

The coefficient of determination was as high as 0.98.

For the same purpose, the SCs of S12, S13 and S15 in 1997–2013, the SCs of S16–20 before engineering construction, and the SCs of S1–8 without S9–11 and S21–22 were selected, and regression analysis was performed using the selected SCs with each section's zonal distance from S1, too. The regression equation was as follow:

$$SC = -33 * Distance + 2396$$

The coefficient of determination was very high (0.95), too.

The regression analysis of ASM and SC with coast's zonal position showed that, after removing the influence of coastal morphology, river course shift and engineering construction, along the northern Yellow River delta, both the ASM and SC had good correlation with the coast's zonal position; when the zonal position moved by each 1 km eastward, the ASM increased by 2.75 m and the SC decreased by 33. The shoreline retreat due to hydrodynamic forces enhanced from west to east gradually, in the northern Yellow River delta.

The numerical simulation results of Lu *et al.* (2011) to the northern Yellow River delta showed that both the wave-current coupled shear stress, wave-induced shear stress and wave-induced liquefaction increase gradually from west to east, and reach maximum at the northeast cape; The measured suspension and tidal current velocity data also showed that, both winter and summer, there existed suspension content and tidal current velocity high value area in the northeastern of Yellow River delta, east gradually increase (Chu *et al.*, 2006; Lu *et al.*, 2011).

Estimation of the erosion area of the northern Yellow River delta

Based on the ASM of each section and the distance between sections, the erosion area can be calculated. For example, the ASMs of S4 and S5 were 12 m and 24.8 m, respectively and their distance is 4.7 km, so, the annual erosion area between S4 and S5 is $(12+24.8)/2/1000 * 4.7 = 0.086$ km^2, the total erosion area between S4 and S5 in 1976–2013 is $0.086 * (2013-1976+1) = 3.3$ km^2.

According to this simple method and based on the proposed ASM in this paper, the total erosion area between S1 and S22 in the northern Yellow River delta was estimated as 197 km^2. The total erosion area influenced by river diversions increased by 32 km^2 in 1976–1996 compared to stable erosion condition in 1997–2013 between S12–15, or 16% of the total erosion area. The erosion area after engineering construction compared to stable erosion condition before engineering construction decreased by 61 km^2, or 31 % of the total erosion area. The erosion area due to RSLC was 9 km^2, or 5% of the total erosion area.

After eliminating the influence of river diversions, engineering construction and RSLC, the total coastal erosion area was 217 km^2, which is mainly caused by the hydrodynamic factors, and it was about 1.1 times of the total erosion area. Therefore, marine hydrodynamic elements such as waves, tides and currents are the main factors to cause the coastal erosion in the northern Yellow River delta.

CONCLUSIONS

(1) Instantaneous shoreline positions of the flat beach in the northern Yellow River delta since 1976 were interpreted based on 222 satellite images. Annual shoreline movements and beach slope coefficients were established through statistical analysis of the instantaneous shoreline positions versus date and water level. In previous studies there were fairly large errors without considering the random errors and water level correlation errors caused by limited and statistically meaningless numbers of satellite images. All these errors are significantly reduced in this study by using aforementioned approach. Thus, through our approach the evaluation of shoreline change for the flat beaches was more reliable and improved much than that in previous studies.

(2) The effect of the Yellow River deltaic course shift on the shoreline change mostly happened in 1976–1996, or in 20 years after the shift. The most intensive affected area was located within 10 km around the Diaokou mouth. The section S13 (3.5 km from the Diaokou mouth) was most affected of all the sections in 20 years by the shift with a retreatment speed rate of 251 m/yr, or by two times more than that in 20 years later. The slope coefficient decreased from 1497 to 987, or 34%, indicating the slope gradient was increasing. The annual shoreline movement and beach slope depended mostly on their distance from the Diaokou mouth, the nearer to the Diaokou mouth, the more erosion rate and slope gradient, and in reverse. However, there were no much changes of the annual shoreline movement and beach slope for the sections outside 10 km from the Diaokou mouth.

River diversions resulting in erosion area increased 32 km^2 in 1976–1996 compared to stable erosion condition in 1997–2013, 16% of the total erosion area. That means the delta was undergoing more intensive erosion in 20 years after the river course shift in 1976.

(3) Coastal engineering constructions lead to slow down the erosion speed of the coast, even stopped the coastal erosion in some areas. Different type of engineering constructions affected coastal erosion differently. Coastal engineering constructions on the northeastern coast can protect the coast from erosion quite effectively. The engineering constructions reduced erosion area of 61 km^2 in 1976–2013, or 31% of the total erosion area.

(4) The shoreline on the flat beaches of S10 – 11 was vulnerable to relative sea-level change, and annual shoreline movement caused by relative sea-level change was 13 m, or 36% of the total average value. The other coast with steep high tide beach was relatively insensitive to relative sea-level change, where the annual shoreline movement caused by relative sea-level change was only 0.5–6 m, or 1–3% of the total average value. The total coastal erosion area of the northern Yellow River delta in 1976–2013 caused by the relative sea-level change was 9 km^2, or 5% of the total erosion area. Relative sea-level change played a minor role in the erosion in the northern Yellow River delta.

(5) The offshore hydrodynamic forces off the northern Yellow River delta gradually increased from west to east along the coast. The value of the annual shoreline movement and the slope were gradually increasing from west to east as well responding to the increasing hydrodynamic forces. The hydrodynamic forces were the weakest in the western area, and the shoreline was basically stable, the annual shoreline movement of S2 in the west was 0 m, indicating the shoreline was stable. The slope coefficient of S1 in the west at low tide was the largest, up to 2 337, indicating the low tide beach of S1 was very gentle. While hydrodynamic forces off the northeast delta protruding corner were the strongest, the beach of S20 in the northeast was steep with reduced slope coefficient down to 249 and fast annual shoreline movement up to 163 m. The annual shoreline movement was increasing by 2.75 m and the slope coefficient was decreasing by 33 as the shoreline position shifted each 1 km eastward, indicating the shoreline erosion speed and steepness were increasing with gradual enhancement of the hydrodynamic forces eastward.

After eliminated the influence of river diversions, engineering construction and RSLC, erosion area influenced by hydrodynamic forces was 217 km^2, roughly equal to the total erosion area. Therefore, the offshore hydrodynamic forces were the major factor for the shoreline change in the northern Yellow River delta.

ACKNOWLEDGMENTS

This study was supported by the National Natural Science Foundation of China (Grant Nos. 41130856, 41206053). We thank anonymous reviewers for their constructive comments and suggestions.

LITERATURE CITED

Bi, N. S.; Wang, H. J., and Yang Z. S., 2014. Recent changes in the erosion-accretion patterns of the active Huanghe (Yellow River) delta lobe caused by human activities. *Continental Shelf Research*, 90, 70–78.

Boak, E. B. and Turner, I. L., 2005. Shoreline definition and detection: a review. *Journal of Coastal Research*, 21 (4), 688–703.

Canny, J. A., 1986. Computational approach to edge detection. *Journal of IEEE Transactions on Pattern Analysis and Machine Intelligence*, 6, 679–698.

Chen, S. L.; Zhang, G. A., and Chen, X. Y., 2006. Coastal Erosion Feature and Mechanism at Feiyantan in the Yellow River delta. *Marine Science Bulletin*, 8(1), 11–20.

Chen, W. W. and Chang, H. K., 2009. Estimation of shoreline position and change from satellite images considering tidal variation. Estuarine. *Coastal and Shelf Science*, 84, 54–60.

Chu, Z. X.; Sun, X. G.; Zhai, S. K., and Xu, K. H., 2006. Changing pattern of accretion/erosion of the modern Yellow River (Huanghe) subaerial delta, China: based on remote sensing images. *Marine Geology*, 227, 13–30.

Church, J. and Gregory, J. M., 2001. Changes in sea-level. In: Houghton, J. T.; Ding, Y.; Griggs, D. J.; Noguer, M.; van der Linden, P. J.; Dai, X.; Maskell, K., and Johnson, C. A. (Eds.), *Climate Change* 2001: *the Scientific Basis. Contribution of Working Group* 1 *to the Third Assessment Report of the Intergovernmental Panel on Climate Change*. Cambridge University Press, Cambridge.

Cui, B. L. and Li, X. Y., 2011. Coastline change of the Yellow River estuary and its response to the sediment and runoff (1976-2005). *Geomorphology*, 127(1), 32-40.

Ekercin, S., 2007. Shoreline change assessment at the Aegean Sea Coasts in Turkey using multi temporal Landsat imagery. *Journal of Coastal Research*, 23, 691-698.

Guariglia, A.; Buonamassa, A.; Losurdo, A.; Saladino, R.; Trivigno, L. M.; Zaccagnino, A., and Colangelo, A., 2006. A multisource approach for coastline mapping and identificationof shoreline changes. *Annals of Geophysics*, 49, 295-304.

Higgins, S.; Overeem, I., and Tanaka, A., 2013. Land subsidence at aquaculture facilities in the Yellow River delta, China. *Geophysical Research Letters*, 40(15): 3898-3902.

Hu, C. H. and Cao, W. H., 2003. Variation, regulation and control of flow and sediment in the Yellow River Estuary: I. Mechanism of flow-sediment transport and evolution. *Journal of Sediment Research*, 5, 1-8. (In Chinese with English abstract).

Huang, H. J. and Fan, H., 2004. Monitoring changes of nearshore zones in the Huanghe (Yellow River) delta since 1976. *Oceanologia ET Limnologia sinica*, 35(4), 306-314. (In Chinese with English abstract)

Kong, D.; Miao, C.; Borthwick, A. G.; Duan, Q.; Liu, H.; Sun, Q., and Gong, W., 2015. Evolution of the Yellow River delta and its relationship with runoff and sediment load from 1983 to 2011. *Journal of Hydrology*, 520, 157-167.

Li, G.; Zhuang, K., and Wei, H. 2000. Sedimentation in the Yellow River delta. Part III. Seabed erosion and diapirism in the abandoned subaqueous delta lobe. *Marine Geology*, 2000, 168(1), 129-144.

Liu, Y. X.; Huang, H. J.; Qiu, Z. F., and Fan, J. Y., 2013. Detecting shoreline change from satellite images based on beach slope estimation in a tidal flat. *International Journal of Applied Earth Observation and Geoinformation*, 23, 165-176.

Lu, J.; Qiao, F. L.; Wang, X. H.; Wang, Y. G.; Teng, Y., and Xia, C. S., 2001. A numerical study of transport dynamics and seasonal variability of the Yellow River sediment in the Bohai and Yellow seas. *Estuarine, Coastal and Shelf Science*, 95, 39-51.

Mason, D. C.; Davenport, I. J., and Flather, R. A., 1997. Interpolation of an intertidal digital elevation model from heighted shorelines: a case study in the western Wash. *Estuarine. Coastal and Shelf Science*, 45, 599-612.

Matsumoto, K.; Takanezawa, T., and Ooe, M., 2000. Ocean tide model developed by assimilating TOPEX/POSEIDON altimetry data into hydrodynamical model: a global and a regional model around Japan. *Journal of Oceanography*, 56, 567-581.

McManus, J., 2002. Deltaic responses to changes in river regimes. *Marine Chemistry*, 79, 155-170.

Milliman, J. D. and Meade, R. H., 1983. World-wide delivery of river sediment to the oceans. *The Journal of Geology*, 91 (1), 1-21.

Milliman, J. D.; Broadus, J. M., and Gable, F., 1989. Environmental and economic implications of rising sea-level and subsiding deltas: the Nile and Bengal examples. *Ambio*, 18, 340-345.

Nilsson, C.; Reidy, C. A.; Dynesius, and Revenga, C., 2005. Fragmentation and flow regulation of the world's large river systems. *Science*, 308, 405-408.

Pang, J. Z. and Si, S. H., 1979. Evolution of the Yellow River mouth: I. Historical shifts. *Oceanologia ET Limnologia Sinica*, 10 (2), 136-141. (In Chinese).

Peng, J.; Chen, S., and Dong, P., 2010. Temporal variation of sediment load in the Yellow River basin, China, and its impacts on the lower reaches and the river delta. *Catena*, 83 (2), 135-147.

Qin, Y. S.; Zhao, Y. Y., and Zhao, S. L., 1985. *The Bohai Sea Geology*. Science Press, Beijing, pp. 61-66. (In Chinese).

Sanchez-Arcilla, A.; Jimenez, J. A., and Valdemoro, H. I., 1998. The Ebro Delta: morphodynamics and vulnerability. *Journal of Coastal Research*, 14, 754-772.

Syvitski, J. P. M.; Vörösmarty, C. V.; Kettner, A. J., and Green, P., 2005. Impact of humans on the flux of terrestrial sediment to the global coastal ocean. *Science*, 308, 376-380.

Wang, B.; Liu, S. Q., and Li, Q., 2006. A real-time contrast enhancement algorithm for infrared images based on plateau histogram. *Infrared Physics & Technology*, 48(1), 77-82.

Wang, H. J.; Bi, N. S.; Saito, Y.; Wang, Y.; Sun, X. G.; Zhang, J., and Yang, Z. S., 2010. Recent changes in sediment delivery by the Huanghe (Yellow River) to the sea: causes and environmental implications in its estuary. *Journal of Hydrology*, 391(3), 302-313.

Yang, G. S., 2002. *The regional response to changing coastal environment in China*. Beijing: Higher Education Press, pp. 60-61 (In Chinese).

Yang, G. S. and Shi, Y. F., 1999. Advances in relative sea level rise and its impacts in the coast of China. *Advances in Earth Science*, 10(5),475-482. (In Chinese).

Yang, Z. S.; Ji, Y. J.; Bi, N. S.; Lei, K., and Wang, H. J., 2011. Sediment transport off the Huanghe (Yellow River) delta and in the adjacent Bohai Sea in winter and seasonal comparison. *Estuarine, Coastal and Shelf Science*, 93, 173-181

Yin, Y. H., 2003. Erosion and silting-up and land-making rates of the modern Yellow River delta coast. *Marine Geology Letters*, 19(7): 13-18. (In Chinese with English abstract)

Yu, J.; Fu, Y.; Li, Y.; Han, G.; Wang, Y.; Zhou, D., and Meixner, F. X. ,2011. Effects of water discharge and sediment load on evolution of modern Yellow River delta, China, over the period from 1976 to 2009. *Biogeosciences*, 8, 2427-2435, 2011

Zang, Q. Y., 1996. *Nearshore sediment along the Yellow River delta*. Ocean Press, Beijing. (In Chinese).

Zhang, J.; Huang, W. W., and Shi, M. C., 1990. Huanghe (Yellow River) and its estuary: sediment origin, transport and deposition. *Journal of Hydrology*, 120 (1-4), 203-223.

Zhou, Y.; Huang, H. Q., and Nanson, G. C., 2015. Progradation of the Yellow (Huanghe) River delta in response to the implementation of a basin-scale water regulation program. *Geomorphology*, 243: 65-74.